Genesis of MgCl2-based Ziegler-Natta Catalysts as Probed with Operando Spectroscopy

(Article begins on next page)

color code is the same as in Figure 1 (25, 60, 90, 120, 150, 200 and 250 °C for $MgCl_2$-MeOH, and 25, 50, 80, 120, 170, 200 and 250 °C for $MgCl_2$-EtOH).

The $MgCl_2$-ROH dealcoholation process was successively followed by means of structural (XRPD) and spectroscopic (DR UV-Vis and DRIFT) methods under *operando* conditions. For each adduct we have defined six temperature steps, corresponding to the most relevant weight losses as determined by TGA (colored dots in Figure 1), at which we have been collecting XRPD patterns and DR UV-Vis spectra, while the DRIFT spectra were collected continuously during the temperature ramp.

Figure 2 shows the evolution of the XRPD patterns during the dealcoholation of the $MgCl_2$-6ROH adducts under N_2 flow at increasing temperatures. In the case of $MgCl_2$-6MeOH (part a), pattern 1, collected at room temperature, is characteristic of a solid solution in which both the Mg^{2+} cations and the Cl^- anions are surrounded by six alcohol molecules in the first solvation shell,[79, 80] thus confirming the stoichiometry resulting from the TGA. In this sense, the structure of the solid $MgCl_2$-6MeOH adduct can be considered as an arrangement of discrete octahedra with Mg^{2+} ions in the centers and MeOH molecules in the corners, and with the chloride ions excluded from the Mg^{2+} coordination sphere as counterions.[81] Upon increasing the temperature, the appearance, transformation and disappearance of several (broad) diffraction peaks are clearly evident and testify the formation of different intermediate crystalline phases as a function of the alcohol content. In particular, the disappearance of the two peaks at 19° and 21° (triangles in Figure 2a) and the appearance of a very weak peak at 12.5° in pattern 4 (star in Figure 2a) are associated with the transition from predominantly solvated ionic structures to covalent $MgCl_2$ long chains, featuring chlorine bridges connecting the Mg atoms.[62, 82] The final XRPD pattern (pattern 7) is that of a layered ŭ-$MgCl_2$ phase characterized by an extensive structural disorder, in agreement with the literature findings,[83, 84] although the sporadic alternation of only partially converted MgCl(OMe) layers cannot be excluded.[60] In particular, the diffraction peak around 2ɗ = 15Å (d = 5.90 Å) corresponds to the (001) basal plane, and its broadness is related to the nano-sized dimensions of the crystalline domains. Moreover, very broad and weak peaks at 2ɗ values around 30-35° and 50° indicate the presence of the catalytically relevant (104) and (110) planes, respectively.[85] For the $MgCl_2$-6EtOH sample, a slower evolution of the XRPD patterns is observed (Figure 2b). The diffraction peaks associated with the intermediate crystalline phases disappear at higher temperatures, in fair agreement with the thermogravimetric profile (Figure 1b). However, the final pattern is the same as that obtained from $MgCl_2$-6MeOH. This is a clear limit of the XRPD technique, which is unable to reveal subtle structural differences for nano-sized and disordered materials.[59]

DR UV-Vis-NIR spectroscopy was applied to monitor the evolution of the electronic properties during the transition from the $MgCl_2$-6MeOH and $MgCl_2$-6EtOH precursors to the activated $MgCl_2$ (Figure 3). The spectra of the starting $MgCl_2$-6ROH adducts (spectra 1 in Figure 3a and b, respectively) show two main bands at ca. 31000 and 38500 cm^{-1}, which are assigned to charge-transfer (CT) transitions involving the Mg^{2+} centers and the ROH ligands, while the bands observed below 10000 cm^{-1} (very narrow) are the overtones and combinations of the vibrational modes of the ROH molecules. Upon dealcoholation, the bands below 10000 cm^{-1} progressively disappear, while the CT bands are gradually modified both in intensity and in position. In particular, a new intense absorption band gradually appears at ca. 42000 cm^{-1}, which is tentatively ascribed to the charge transfer transition from a Cl^- ligand to a highly uncoordinated Mg^{2+} center, in analogy to what reported by Zecchina et al. for defects on MgO.[86] A second envelope of bands is detectable in the final spectrum (spectrum 7) at 33000 and 23500 cm^{-1}, which are responsible for the goldenrod yellow color of the samples and are compatible with the presence of trapped electrons, i.e. color centers.[87] This phenomenon is more pronounced for the $MgCl_2$-$EtOH_{-250}$ sample (Figure 3b). These bands are not affected by the successive adsorption of molecules (including H_2O), suggesting that the color centers are buried in the bulk of the $MgCl_2$ (and hence not relevant to the catalysis).

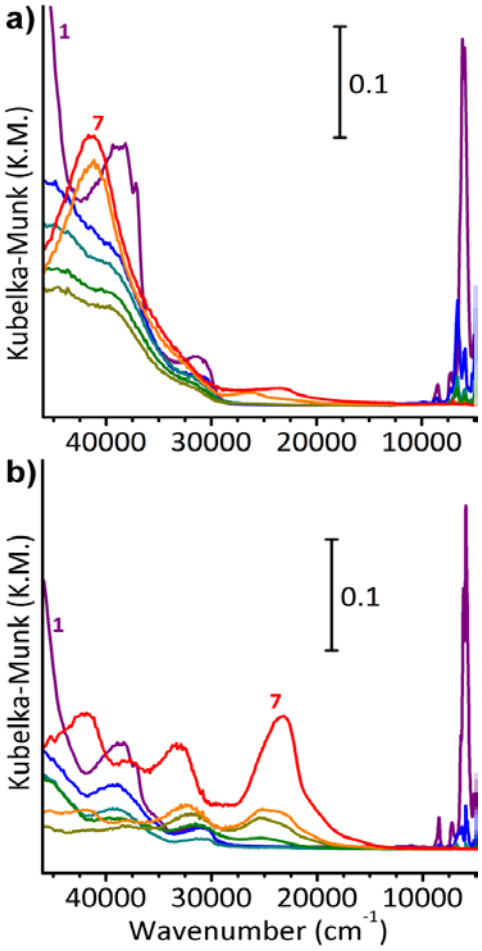

Figure 3. Evolution of the diffuse reflectance (DR) UV-Vis spectra upon dealcoholation of $MgCl_2$-6MeOH (part a) and $MgCl_2$-EtOH (part b), under N_2 flux (20 mL/min) at increasing temperatures (2 °C/min), from 25 to 250 °C. The color code is the same as in Figure 1 (25, 60, 90, 120, 150, 200 and 250 °C for $MgCl_2$-MeOH, and 25, 50, 80, 120, 170, 200 and 250 °C for $MgCl_2$-EtOH).

Finally, Figure 4 shows the evolution of the DRIFT spectra during the dealcoholation of $MgCl_2$-6ROH at increasing temperature. In the case of $MgCl_2$-6MeOH (Figure 4a), the initial spectrum is dominated by the absorption bands of the methanol molecules entangled within the material. The spectrum of liquid methanol (reported in Figure 4a for the sake of comparison) is characterized by the ɜ(OH) band at 3330 cm^{-1}, the asymmetric and symmetric ɜ(CH_3) at 2943 and 2832 cm^{-1}, the ŭ(CH_3) at 1450 cm^{-1}, the ŭ(OH) at 1420 cm^{-1}, $ŭ_{rocking}$(OH) at 1115 cm^{-1}, the ɜ(C-O) at 1022 cm^{-1}, and a very weak and broad band at 2600-2500 cm^{-1} including several combinations of the bending and rocking modes.[88] In the ɜ(OH) region, the spectrum of $MgCl_2$-6MeOH is very similar to that of liquid methanol. This is in agreement with the NMR data reported by Butler et al., indicating that the MeOH molecules in the solvation shell of Mg halides are perturbed in a similar way as the MeOH molecules in the liquid phase.[89]

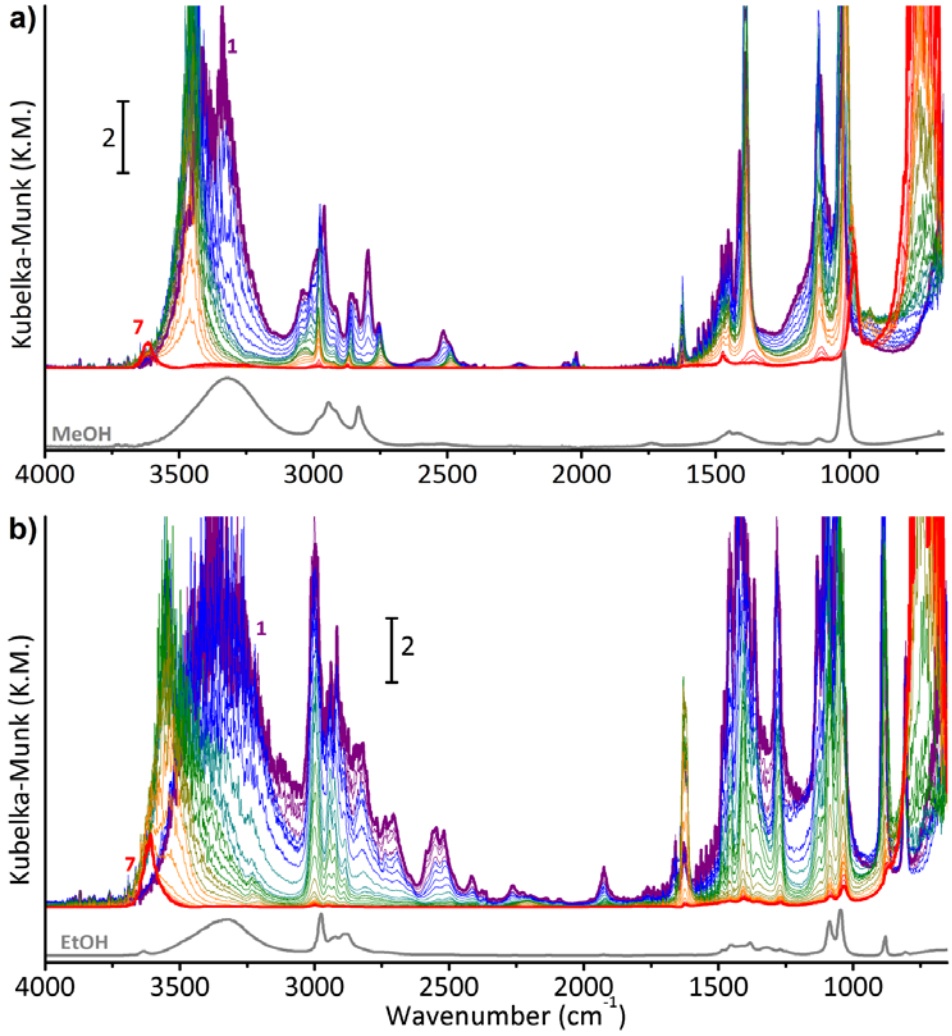

Figure 4. Evolution of the diffuse reflectance infrared Fourier transform (DRIFT) spectra upon dealcoholation of $MgCl_2$-6MeOH (part a) and $MgCl_2$-EtOH (part b), under N_2 flux (20 mL/min) at increasing temperatures (2 °C/min), from 25 to 250 °C. The color code is the same as in Figure 1 (25, 60, 90, 120, 150, 200 and 250 °C for $MgCl_2$-MeOH, and 25, 50, 80, 120, 170, 200 and 250 °C for $MgCl_2$-EtOH). Both sequences of DRIFT spectra are compared with the spectra of respective liquid alcohols collected in attenuated total reflectance (ATR) mode.

In the ɜ(CH_x) region, the bands due to the asymmetric and symmetric ɜ(CH_3) modes are more spaced to each other (at 2960 and 2795 cm^{-1}) because of the interaction with the Cl^- counterions, and three new bands are present at 2980, 2867 and 2750 cm^{-1}. The three bands are respectively assigned to the asymmetric and symmetric ɜ(CH_3) and to the overtone of the ŭ(CH_3) for methoxy ligands coordinated to the Mg^{2+}.[90, 91] During the dealcoholation process, the ɜ(OH) band reduces in intensity and progressively shifts up-ward to ca. 3620 cm^{-1}, because of the continuous loss of the H-bonding interaction among the alcohol molecules in the coordination sphere of the Mg^{2+} ions. In the ɜ(CH_x) region, the spectra gradually simplify, and the bands associated to the methoxy species are the only ones remaining in the final spectrum, although with a very low intensity. As a

matter of fact, spectrum 7 is characterized by a very low absorption in the whole spectral range (as expected, since neat $MgCl_2$ should be completely transparent in the Mid-IR region). The few residual bands indicate the persistence of a small number of alcohol-derived moieties, strongly bound to the $MgCl_2$. The most intense band (out-of-scale in DRIFT) is centered around 750 cm^{-1}, and indicates the formation of Mg-O covalent bonds. These results are in good agreement with the recent findings, which pointed out the formation of methoxy groups during the synthesis of methanol-shaped Ziegler-Natta catalysts through the thermal deprotonation of the outgoing MeOH molecules.[92] Finally, it should be also noted that a weak band at 1620 cm^{-1} starts growing during the first steps of the dealcoholation, but rapidly decreases at temperatures above 120 ÁC. This band is assigned to the ŭ(OH) vibrational mode of physisorbed water,[91] which derives from very small impurities in the N_2 flux despite the optimization of the experimental setup. This adventitious water cannot adsorb until the $MgCl_2$ surface is covered by the alcohol and is easily removed at temperatures above the boiling point.

An analogous sequence of DRIFT spectra was also observed upon dealcoholation of the $MgCl_2$-6EtOH adduct (Figure 4b). Also in this case the first spectrum is dominated by the spectroscopic manifestations of the pure alcohol, whereas the last spectrum presents only a few bands due to residual ethoxy byproducts, whose formation has already been assessed in literature.[66, 93]

The whole set of experimental data discussed in this section converges in showing that the stepwise dealcoholation of the $MgCl_2$-6ROH adducts occurs through the formation of a large number of intermediate species (some of them crystalline) and following a series of side reactions often neglected in the specialized literature. The slightly different evolution of the two alcoholate precursors may explain the different properties of the produced $MgCl_2$, in terms of specific surface area, particles size and morphology.[58, 59, 94, 95]

Genesis of the active sites on $MgCl_2$

The reactions of the high surface area $MgCl_2$ with $TiCl_4$ and TEA, leading to the active Ziegler-Natta catalyst, were followed by *operando* DR UV-Vis and DRIFT spectroscopic techniques. Qualitatively, no significant differences are observed between the spectra collected on the sample derived from the $MgCl_2$-6MeOH and the spectra collected on the sample derived from the $MgCl_2$-6EtOH, indicating that the different precursors affect only the content and the distribution of the Ti centers, but not their intrinsic properties.

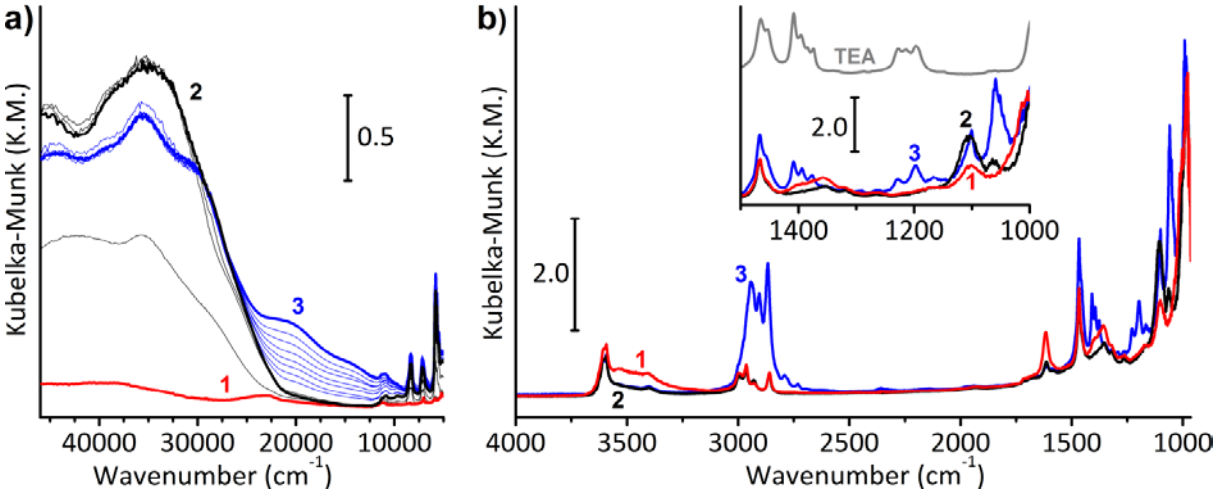

Figure 5. Evolution of the *operando* diffuse reflectance (DR) UV-Vis-NIR (Part a) and diffuse reflectance infrared Fourier transform (DRIFT) (Part b) spectra upon titanation of $MgCl_{2\text{-}250}$ at 90 °C with injections of hexane-diluted $TiCl_4$ in N_2 flux (from spectrum 1 to spectrum 2), and upon activation of $MgCl_{2\text{-}250}$/$TiCl_{4\text{-}90}$ at 25 °C with injections of hexane-diluted TEA in N_2 flux (from spectrum 2 to spectrum 3). Inset of part b shows a magnification of the DRIFT spectra in the 1500-1000 cm^{-1} region; the spectra are compared with the spectrum of liquid triethylaluminum (TEA) collected in attenuated total reflectance (ATR) mode.

Upon dosage of a stoichiometric amount of $TiCl_4$ at 90 °C, two intense absorption bands at 42000 and 35500 cm^{-1} (with a well-defined shoulder at 28000 cm^{-1}) appear in the DR UV-Vis spectrum (spectrum 2 in Figure 5a). These bands are assigned to charge transfer transitions from the Cl ligands to the Ti metal centers of the newly formed $TiCl_x$ species. According to the Jorgensen rules on the optical electronegativities of transition metals and their ligands,[96, 97] the band at 28000 cm^{-1} is univocally ascribed to 6-fold coordinated Ti^{4+} sites, while at higher wavenumbers also 4-fold coordinated Ti^{4+} sites give a contribution.[98] Interestingly, the band at 28000 cm^{-1} has a slightly slower dynamics than the other bands. This observation can be related to an initial step of physisorption of $TiCl_4$, which is arranged in tetrahedrons both in the liquid and vapor phases, followed by chemisorption in a more stable configuration, where Ti centers assume an octahedral geometry, as well established in the literature.[44, 99-102] This spectral sequence is in agreement with the observations of Brambilla et al. for ball-milled $MgCl_2$-$TiCl_4$ complexes.[103] On the contrary, a few changes are observed upon titanation of $MgCl_{2\text{-}250}$ in the MIR region

(spectrum 2 in Figure 5b). A slight decrease of the ɜ(OH) absorption band at around 3500 cm^{-1} indicates that $TiCl_4$ reacts with residual alcohol-derived species and/or with traces of adventitious H_2O on $MgCl_2$ surface. Such a reaction is also accompanied by the appearance of a very weak band at around 1100 cm^{-1} (clearly visible in the inset), which is attributed to the formation of Ti alkoxide byproducts.[104]

During the activation with TEA at 25 °C, an extensive absorption slowly appears in the DR UV-Vis spectra in the d-d region (from spectrum 2 to 3 in Figure 5a), showing the reduction of the Ti^{4+} centers to Ti^{3+}.[98] In particular, two bands are distinguishable at 21000 and 14500 cm^{-1}. These bands are quite broad and relatively intense (ca. 1 K.M. unit), despite the low concentration of Ti (1 wt%), suggesting that most of the Ti^{3+} sites are not isolated but rather aggregated into small clusters, as it was first proposed by Brant and Speca on the base of quantitative EPR measurements.[105, 106] As a matter of fact, such a spectrum resembles those of the violet Ŭ and ɔ-$TiCl_3$,[16, 98, 107] which present two intense bands at 18300 and 13800 cm^{-1}. The latter band is ascribed to an intersite $^2T_{2g}$ Ÿ ^2E_g d-d transition involving two Ti^{3+} sites bridged by a Cl ligand, thus gaining intensity from the Cl Ÿ Ti CT transition at higher energy.[108] The slight blue-shift to higher wavenumbers of the $MgCl_{2\text{-}250}/TiCl_{4\text{-}90}$/TEA spectrum with respect to that of bulk $TiCl_3$ can be explained in terms of the smaller sizes of the $TiCl_x$ aggregates, but it is also compatible with the presence of alkyl ligands in the coordination sphere,[109] in accordance with the spectrochemical series of the ligands.[110] It is worth noticing that the DR UV-Vis spectra shown in Figure 5a neither exclude the presence of isolated Ti^{3+} sites (that should contribute at around 12000 cm^{-1},[108] or higher if alkylated,[111, 112] but with a much weaker intensity), nor the presence of over-reduced Ti^{2+} sites (that should contribute in an extended spectral range, but with a very weak intensity).[113-115] We are tempted to exclude Ti over-reduction on account of the low amount of TEA used during the experiment (Al:Ti=2:1),[116] but the co-presence of both isolated $TiCl_x$ species and Ti clusters, each one expressing a specific activity,[117] is plausible and cannot be discarded at all.

DRIFT spectra upon TEA dosage in Figure 5b are dominated by the absorption bands of the hexane solvent, but they are no more present in the final spectrum after flushing the cell with N_2 (spectrum 3). In that spectrum TEA dosage is testified by the appearance of some absorption bands in the ɜ(CH_x) (2950ī2800 $cm^{ī1}$) and ŭ(CH_x) (1500ī1350 $cm^{ī1}$) regions, which are related to the vibrational modes of the alkyl chains deriving from TEA. These bands are very similar to the fingerprints of pure TEA (inset in Figure 3b),[118] and account for the coexistence of alkylated $TiCl_xR_y$ species, AlR_xCl_y byproducts, and unreacted AlR_3, as already observed for other Ziegler-Natta catalysts.[119, 120] Unfortunately, a clear distinction among all the different species could not be addressed here. Finally, a few changes are observed in the range between 1100 and 1000 cm^{-1}, likely associated to the reaction of TEA with the above mentioned Ti alkoxide species.

Ethylene polymerization

The activity of the $MgCl_{2\text{-}250}/TiCl_{4\text{-}90}$/TEA catalyst towards ethylene polymerization was tested by contacting the catalyst with ethylene (20 mL/min, 25 % of C_2H_4 in N_2) at room temperature and atmospheric pressure. Under these conditions, the catalyst is quickly submerged by a thick layer of polyethylene. This is well-evident in Figure 6, which shows the picture of the sample in the DRIFT cell before (part a) and after (part b) ethylene polymerization (10 minutes). The powder enormously increases in size, up to an overflow from the sample holder. As a consequence, no significant information can be achieved anymore by DR UV-Vis spectroscopy, because such a polymer coating changes the light scattering properties of the catalyst particles under study, shielding the catalytic sites from the incident light and negatively affecting the overall absorbance of the spectra, as clearly illustrated by Barzan et al. when studying ethylene polymerization on the Phillips catalyst.[26] The occurrence of ethylene polymerization is also clear by evaluating the evolution of the DRIFT spectra in Figure 6c, analogously to what recently observed on industrial catalysts.[112] After flushing the cell with pure N_2 to remove from the spectra the roto-vibrational contributions of gaseous ethylene (centered at 3105, 2990 and 1445 cm^{-1}), spectrum 3 in Figure 6c is dominated by the signals of growing polyethylene, that are the off-scale asymmetric and symmetric ɜ(CH_2) and ŭ(CH_2) modes (at around 2920, 2855 and 1470 cm^{-1}, respectively), and the very weak overtones and combinations (e.g., $ɜ_{asym}(CH_2)$+ŭ(CH_2) and $ɜ_{sym}(CH_2)$+ŭ(CH_2) at 4320 and 4250 cm^{-1}, respectively), further demonstrating the formation of polyethylene by the catalyst system under study.[121, 122]

Figure 6. Parts a and b) Pictures of the $MgCl_{2\text{-}250}/TiCl_{4\text{-}90}$/TEA catalyst within the Harrick Praying Mantis diffuse reflectance infrared Fourier transform (DRIFT) cell before and after ethylene polymerization. Part c) Evolution of the *operando* FT-IR spectra upon ethylene polymerization (N_2:C_2H_4 = 75:25, 20 mL/min) on the

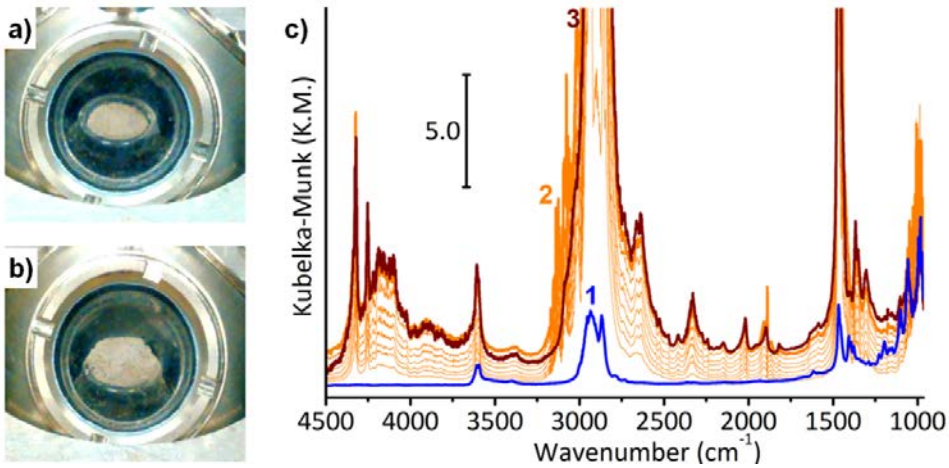

$MgCl_{2\text{-}250}/TiCl_{4\text{-}90}$/TEA catalyst (from spectrum 1 to spectrum 2) and after flushing the cell with pure N_2 flux (spectrum 3). The spectra upon ethylene polymerization were collected every minute for 10 minutes.

Conclusions

The individual steps for the synthesis of a Ziegler-Natta catalyst were successfully monitored, pointing out all the intermediate transitions that could not have been detected otherwise, but are crucial for the final composition of the catalyst. Although the adopted procedure is unusual for the industrial practice, where most of the reactions take place all at once within the reactor, some important remarks were achieved on the genesis of the Ziegler-Natta catalysts. The dealcoholation of $MgCl_2$-nMeOH and $MgCl_2$-nEtOH adducts to arrive at a high-surface area $MgCl_2$ evolves through a considerable number of intermediate phases (some of them which are found to be crystalline), resulting in the formation of alcohol-derived by-products strongly bound to the material. Such an observation substantiate the different properties reported in literature for $MgCl_2$ derived from different alcoholate precursors. Then, the titanation of the so formed $MgCl_2$ support material appears to be divided into two sequential steps, in which $TiCl_4$ is first physisorbed onto the surface and then strongly chemisorbed on $MgCl_2$. Finally, the activation of the pre-catalyst by triethylaluminum clearly causes the formation of Ti clusters through the partial aggregation of the surface $TiCl_x$ species, although the concurrent presence of isolated Ti centers cannot be discarded. The resulting Ziegler-Natta catalyst, synthesized through a surface science approach, presented a valuable activity towards ethylene polymerization, hence it can be considered as representative for industrial catalysts.

The reported data clearly demonstrate that *operando* spectroscopy allow appreciating transient details, that otherwise would not be revealed. Such information can be complementary with the fundamental studies under static conditions already present in literature, highlighting expediencies and criticalities intrinsic to the catalytic process, but which are often neglected. In this way it is possible to acquire a more complete knowledge of Ziegler-Natta catalysis.

Experimental Section

Materials Synthesis

Anhydrous $MgCl_2$ powder (Ó99%), methanol (99.8%) and ethanol (Ó99.8%), toluene (99.8%), hexane (95%), $TiCl_4$ (99.9%), and triethylaluminum (TEA, 93%) were used as received from Sigma-Aldrich. All the compounds were handled in a glove-box and treated under N_2 flux (>99.998%, Rivoira), in order to avoid possible contaminations. Solvents were dried under activated molecular sieves.

All experimental steps are summarized in Scheme 1 and described in detail in the following paragraphs.

The $MgCl_2$-nROH adducts were synthesized through an azeotropic distillation method (step a in Scheme 1), stirring for 3 h at 95 °C under inert atmosphere a solution of $MgCl_2$ in alcohol (either methanol or ethanol, 12 mL per gram of $MgCl_2$) and toluene, according to a procedure well established in the literature,[78, 123] and in the same way as reported in previous works.[45, 59] At the end of the process, the precipitation of the $MgCl_2$-nCH_3OH or $MgCl_2$-nCH_3CH_2OH powders occurred, in agreement with the $MgCl_2$ solubility models proposed by Zeng et al.[124]

The controlled dealcoholation of the $MgCl_2$-nROH adducts (step b) was achieved in N_2 flux (20 mL/min), heating the samples with a temperature ramp of 2 °C/min up to 250 °C, followed by 30 min of isotherm at the same temperature. The final temperature of this thermal treatment was chosen on the basis of the thermogravimetrical analysis (TGA), to assure the complete removal of all the alcohol molecules. The activated high-surface area $MgCl_2$ will be referred to as $MgCl_{2\text{-}250}$.

For the titanation of activated $MgCl_2$ (step c), a stoichiometric amount of $TiCl_4$, necessary for achieving a final Ti content of 1 wt%, was diluted in hexane (50 % v/v in hexane) and injected through a septum in the N_2 flux (20 mL/min). Then the $TiCl_4$ vapors reach with the activated $MgCl_2$ at 90 °C. The employed setup is similar to that described in previous work.[27] The final amount of titanium that is grafted on $MgCl_2$ with this procedure is close to 1.0 wt%, as determined by ICP analysis.[45] The so formed pre-catalysts will hereafter be referred to as $MgCl_{2\text{-}250}/TiCl_{4\text{-}90}$.

The activation of the $MgCl_{2\text{-}250}/TiCl_{4\text{-}90}$ pre-catalyst (step d) was accomplished by using a diluted solution of TEA (1.25 M in hexane), attaining an average Ti:Al stoichiometry of 1:2, with respect to the total $TiCl_4$ injected. TEA was dosed at room temperature, following the same procedure described for $TiCl_4$ dosage. The resulting active catalyst will be referred to as $MgCl_{2\text{-}250}/TiCl_{4\text{-}90}$/TEA.

Both $TiCl_4$ and TEA dosages are followed by a mild washing of the catalyst by injecting some pure solvent into the N_2 flux through the sample.

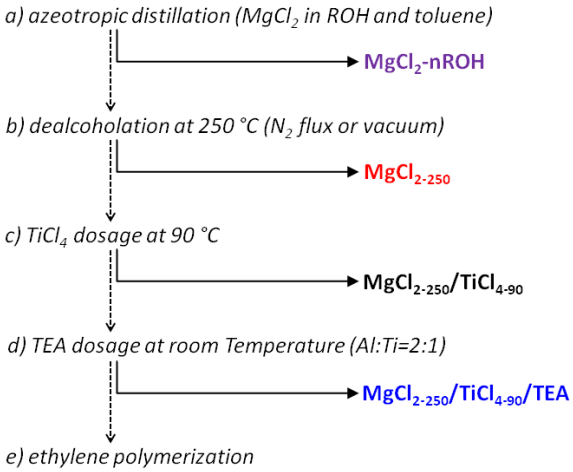

Scheme 1. Sequence of the experimental steps for the whole catalytic process under examination. All stages are labeled as in the main text, following the same color code in the next figures.

Ethylene polymerization (step e) was performed flowing through the measurement cell at 20 mL/min a 75:25 mixture of N_2 and C_2H_4 (>99.9%, Linde), at room temperature and atmospheric pressure.

Materials Characterization and Testing

Thermogravimetric analysis (TGA) measurements during the $MgCl_2$-nROH dealcoholation were performed with a TA Q600 instrument at a heating rate of 2 °C/min in a temperature range between 30 and 300 °C,